

Dynamics of stripes in doped antiferromagnets

C. Morais Smith and Yu. A. Dimashko

I Institut für Theoretische Physik, Universität Hamburg, D-20355 Hamburg, Germany

N. Hasselmann

*I Institut für Theoretische Physik, Universität Hamburg, D-20355 Hamburg, Germany
and Department of Physics, University of California, Riverside, California 92521*

A. O. Caldeira

Instituto de Física Gleb Wataghin, Universidade Estadual de Campinas, CP 6165, 13085-970 Campinas SP, Brazil

(Received 6 November 1997)

We study the dynamics of the striped phase, which has previously been suggested to be the ground state of a doped antiferromagnet. Starting from the t - J model, we derive the classical equation governing the motion of the charged wall by using a fictitious spin model as an intermediate step. A wavelike equation of motion is obtained and the wall elasticity and mass density constants are derived in terms of the t and J parameters. The wall is then regarded as an elastic string that will be trapped by the pinning potential produced by randomly distributed impurities. We evaluate the pinning potential and estimate the threshold electric field that has to be applied to the system in order to release the walls. Besides, the dynamics of the stripe in the presence of a bias field below the threshold is considered and the high- and low-temperature relaxation rates are derived. [S0163-1829(98)00625-0]

I. INTRODUCTION

The discovery of a deep connection between superconductivity and quantum antiferromagnetism in the phase diagram of the cuprate perovskites has stimulated various attempts to understand the effects of dilute holes in a spin- $\frac{1}{2}$ Heisenberg antiferromagnet. The problem has usually been addressed by assuming that a doped antiferromagnet can be described by a gas of holes with uniform density. However, several calculations¹⁻⁷ suggest that in this system there is a modulation of the charge and spin densities, i.e., the holes cluster along lines that separate undoped antiferromagnetic domains (striped phase).

Experimentally, recent measurements also indicate that striped order indeed occurs in doped planar antiferromagnets. In the insulating nickel oxides, such stripe modulations were reported⁸⁻¹⁰ and the data were consistent with multi-band Hubbard model calculations.¹¹ For the case of the copper oxides, elastic neutron-diffraction experiments have revealed static stripe order in the superconductivity suppressed compound $\text{La}_{1.48}\text{Nd}_{0.4}\text{Sr}_{0.12}\text{CuO}_4$ (Ref. 12) while in the superconducting compound $\text{La}_{2-x}\text{Sr}_x\text{CuO}_4$ inelastic scattering peaks at incommensurate wave vectors suggest the existence of a very similar, albeit slowly fluctuating, striped phase.^{13,14} Although incommensurate spin fluctuations are not observed in the low doping region of the cuprates, muon spin resonance and nuclear quadrupole resonance experiments on $\text{La}_{2-x}\text{Sr}_x\text{CuO}_4$ with $0 \leq x \leq 0.018$ (Ref. 15) have been successfully interpreted within models that presume a striped structure.¹⁶ The surprisingly strong suppression of superconductivity in these materials for even low Zn doping was also found to be consistent with the existence of stripes.¹⁷

The objective of the present work is to study the dynamics of this striped phase in the low doping regime, where inter-

actions between neighboring stripes are assumed to be negligible. We treat the problem on the basis of the t - J model and establish the connection to the discrete elastic theory. The domain wall is then considered from a phenomenological point of view, i.e., as an elastic line trapped by the pinning potential produced by impurities. The depinning of the line from the potential well by applying an electrical field perpendicular to the stripe structure is investigated, and the threshold field corresponding to the onset of a state with mobile lines is determined. Finally, the relaxation process in the presence of a bias field below the threshold is considered and the classical and quantum decay rates from the metastable state are computed.

The first calculations of the striped phase in two-dimensional (2D) antiferromagnets with holes have been done within the Hubbard model in the vicinity of half filling. They were based on the self-consistent Hartree-Fock formalism and have been performed for small and large values of the ratio U/t . The results can be summarized as follows: In the small U approximation, vertical domain walls (parallel to the x or y axis) are stable,^{1,3} whereas for large U diagonal walls are energetically more favorable.^{2,3} This crossover from vertical to diagonal stripes was numerically calculated to happen at $U/t \sim 3.6$ (Ref. 3) (see Fig. 1).

In the $U/t \gg 1$ limit, the Hubbard model with an almost half-filled band can be reduced to the t - J model with an effective exchange constant $J = 4t^2/U$.¹⁸ Contrary to the Hubbard model, where each site of the lattice corresponds to four possible states, in the t - J model only three states are allowed, since double occupancy is forbidden. Hence, the dimensionality of the Hilbert space in the latter model is much smaller and for finite clusters an exact diagonalization of the system, without using the Hartree-Fock approximation, is possible. These studies of the t - J model have been

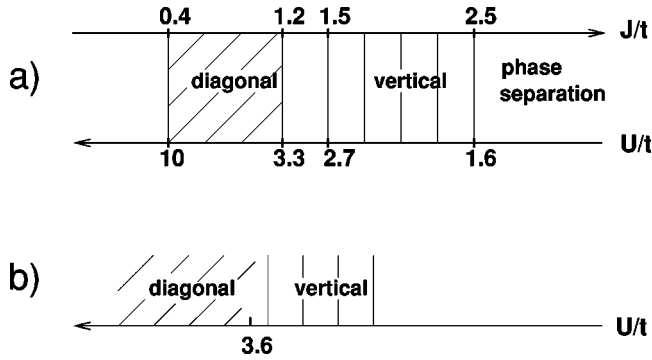


FIG. 1. Regions corresponding to the diagonal and vertical striped phase obtained from (a) exact diagonalization in small systems (Ref. 7); (b) Hartree-Fock calculations (Ref. 3).

recently performed and they confirm the results obtained previously: By exactly diagonalizing small systems, Prelovsek and Zotos⁷ have verified that a striped phase with holes forming domain walls along the (0,1) or (1,0) direction arises for $J > J_s \sim 1.5t$, while in the regime $0.4 < J/t < 1.2$ the domain walls appear along the (1,1) direction. Besides, they found signs of phase separation into a hole-rich and a hole-free phase at $J > J_s^* \sim 2.5t$. In Fig. 1 we graphically represent the results obtained from the t - J and Hubbard models to allow for a direct comparison between them.

The results obtained for the striped phase can be understood on simple physical grounds. In Figs. 2(a) and 2(b), diagonal and vertical stripes (ensemble of holes) embedded in an antiferromagnetic (AF) background are, respectively, represented. The holes can jump from one site to another and during this process they gain kinetic energy t . An inspection of Fig. 2 leads us to conclude that the diagonal configuration favors the dynamics (in this case the holes can move in 2D, horizontally or vertically), whereas for the vertical stripe the holes are confined to move only in the horizontal direction. On the other hand, the vertical configuration breaks fewer AF bonds and hence there is a gain in the exchange energy J . Then, the final behavior that results from the competition between the kinetic (t) and the exchange (J) energies (see Fig. 2) is as follows. When $t > J = 4t^2/U$, i.e., for U/t large, the kinetic energy dominates over the exchange energy and the stripes are diagonally arranged. When the gain in the exchange energy becomes more relevant, for $t < J$, the vertical (horizontal) formation arises.

Besides the question concerning the orientation of the stripes (vertical/horizontal or diagonal), another essential, yet controversial, point about the domain-wall structure emerges: the width and the composition of the walls. Neutron-scattering experiments suggest that single chains

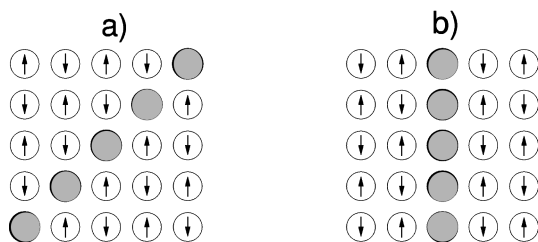


FIG. 2. (a) Diagonal and (b) vertical stripe configurations.

composed of one hole per two lattice sites should separate AF antodomains.¹² On the other hand, Hartree-Fock calculations¹⁻⁴ and exact diagonalization in small clusters⁷ predict a domain-wall filling of one hole per unit cell. Recent numerical density-matrix renormalization-group results show domain walls composed of a double chain of holes (bond-centered structures), or a triple chain of holes (site-centered structures), depending on the boundary conditions and on the dimensions of the clusters.¹⁹ Here, we concentrate on the simplest possibility: a domain wall composed of one hole per site separating AF antodomains. Although this structure seems to be more plausible for describing the nickelates (the cuprate strings should be metallic; hence, with one hole per two sites), we still apply our results to estimate the values for a cuprate material.

Recently, the stripe dynamics have been studied from a different perspective: the domain walls were regarded from a phenomenological point of view as vibrating strings.²⁰ The motion of a single stripe was initially considered, and the analysis was then extended to the more complicated regime involving many (interacting) domain walls. Here, we adopt a similar description. However, instead of using the initial assumption that the stripe can be described by an elastic line, we start from the t - J model and show that the classical equation of motion describing the stripe dynamics in the limit of long-wavelength displacements has a wavelike form. In this way, we deduce the phenomenological mass and elastic coefficients for the string in connection with the “microscopic” t and J parameters. Without loss of generality, we concentrate on the vertical configuration. This implies that our considerations hold for $J_s^* > J > J_s$, i.e., $2.5t > J > 1.5t$.⁷ On top of that, we study the problem in the dilute limit, when the doping concentration is low and we can investigate the behavior of a single stripe (chain of holes).

In order to derive the quantum equation of motion describing the dynamics of the n th hole in the chain, we map the initial t - J Hamiltonian onto a quantum spin-chain problem with large spin. Replacing the spin-chain operators in the quantum equation of motion by their classical values and considering the long-wavelength limit, a classical wave-type equation of motion is derived for the stripe. The justification for this classical approach rests on the assumption of the existence of zero mode excitations, i.e., we assume that a continuum description of the problem is possible and that the discreteness of the original lattice formulation is irrelevant in the long-wavelength limit. Recently, it was shown²¹⁻²³ that the striped phase undergoes a roughening transition, i.e., the flat (gapped) phase present at higher values of J/t becomes rough (gapless) as J/t is reduced. Hence, our approach applies to the rough phase of the stripe, in which the underlying lattice structure is unimportant and the behavior of the system is governed by a Gaussian fixed point.

Since the equation of motion describing the stripe dynamics has a wavelike form, the stripe is from then onwards regarded as an elastic string. The random pinning potential due to the presence of impurities is evaluated and the activation energy barrier is calculated for the case of a bias electric field applied perpendicularly to the stripe, both in the high-temperature phase, where quantum fluctuations can be neglected, and in the quantum dominated low-temperature phase. The threshold field is estimated and we briefly discuss

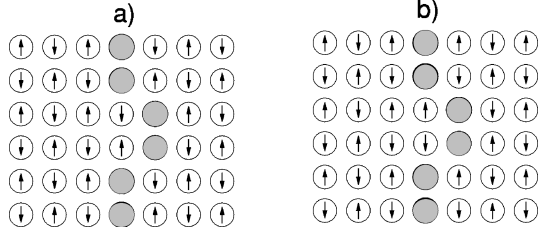


FIG. 3. (a) Delocalized stripe (antiphase domain boundary); (b) localized stripe (hypothetical case corresponding to a phase domain boundary).

if and how stripe depinning could be experimentally observed. The dissipation effects are also considered and their influence in the stripe depinning is discussed.

The outline of the paper is as follows. In Sec. II, the model is introduced and the equation of motion is derived. The pinning potential and the threshold field are calculated in Sec. III. In Sec. IV we investigate the classical and quantum relaxation regimes at fields below the threshold. The discussions and conclusions are presented in Sec. V.

II. THE MODEL

The t - J Hamiltonian describing a chain of holes (stripe) embedded in an antiferromagnetic background is¹⁸

$$H_{tJ} = -t \sum_{\langle ij \rangle} c_{i\sigma}^\dagger c_{j\sigma} + J \sum_{\langle ij \rangle} \left(\vec{S}_i \cdot \vec{S}_j - \frac{1}{4} n_i n_j \right). \quad (1)$$

Here, H_{tJ} acts in the truncated Hilbert space consisting of states for which the double occupancy of any site is forbidden, i.e., $n_i = 0, 1$.

We apply this Hamiltonian for investigating the dynamics of an infinitely long stripe. The linear concentration of holes along the stripe is assumed to be one hole per lattice point, so we can neglect charge and spin fluctuations along the stripe. The stripe represents a domain boundary (DB) dividing the antiferromagnetic plane into two Néel phases. We consider these two phases to have opposite staggered magnetization (*antiphase* DB). Hence, the string can move without disturbing the initial magnetic order, i.e., it is delocalized [see Fig. 3(a)]. This case is opposite to the other hypothetical case, when these two staggered fields are equivalent (*phase* DB) and the string is localized, since its motion is strongly frustrated by the surrounding magnetic order [Fig. 3(b)].

Here we concentrate on the dynamics of the vertical configuration and assume that the stripe is located along the y direction. Furthermore, we make one additional hypothesis, which reduces the problem to a directed, but discrete, polymer problem: the holes are constrained to move along the transversal x direction only, i.e., we neglect overhangs. This assumption is true for the shortest excursions of the holes from the initial vertical position of the string (up to one step) and therefore seems to be plausible as far as one considers only small magnitudes of the oscillations. Therefore, the supposition holds for the $J > t$ case, when larger excursions of the holes are suppressed by the dominating exchange J term. In the opposite $J < t$ case, the hypothesis ceases to be valid, and the one-dimensional approximation cannot be used any-

more. This corresponds to the more complicated case of the diagonal DB, which will be treated in a separate work.

Let us denote u_n the displacement of the n th hole from its equilibrium position along the x direction. We describe the relative displacement of two neighboring holes by $\sigma_n^z = u_n - u_{n-1}$ and treat this value as the z component of some effective local spin $\vec{\sigma}_n$. This spin is related to the n th segment of the stripe. Displacement of the n th hole by one step along the positive direction of the x axis increases σ_n^z ($\sigma_n^z \rightarrow \sigma_n^z + 1$) and decreases σ_{n+1}^z ($\sigma_{n+1}^z \rightarrow \sigma_{n+1}^z - 1$). Their sum remains unchanged. Hence, the motion of the n th hole is described by the spin operator $-t\sigma^{-2}(\sigma_{n+1}^+ \sigma_n^- + \sigma_{n+1}^- \sigma_n^+)$. The σ^{-2} factor provides the conservation of the norm under the action of this term on the spin-wave function. Moreover, by accounting for the different Néel order to the left and right of the stripe, we see that any increase of the relative displacement of two neighboring holes by unity results in an increase of the exchange energy by $J/2$. Thus, the contribution of the n th segment to the exchange energy of the string is $(J/2)|\sigma_n^z|$.

A similar problem was investigated by Eskes *et al.*,²² but the Hilbert space in their work was truncated in a different way. Only configurations where two neighboring holes are separated by one lattice unity were allowed. Hence, they mapped the relative displacement coordinate onto a spin-one chain and determined the phase diagram features, in the same spirit as in Refs. 23 and 24. Here, we consider a broader Hilbert space and search for the classical equations of motion instead of the quantum phase diagram.

The projection of the initial t - J Hamiltonian onto the new Hilbert space gives rise to the spin-chain problem with the effective Hamiltonian

$$H = -\frac{t}{\sigma^2} \sum_n (\sigma_{n+1}^+ \sigma_n^- + \sigma_{n+1}^- \sigma_n^+) + \frac{J}{2} \sum_n |\sigma_n^z| \quad (2)$$

and the standard commutation relations

$$[\sigma_n^z, \sigma_m^\pm] = \pm \delta_{n,m} \sigma_m^\pm, \quad [\sigma_n^+, \sigma_m^-] = 2 \delta_{n,m} \sigma_m^z.$$

The effective spin σ is the maximal relative displacement of two neighboring holes.

The configuration of the stripe is determined by the z projection of the spin, σ_n^z . The quantum equation governing the motion of the σ_n^z operator is

$$\hbar^2 \ddot{\sigma}_n^z = -[[\sigma_n^z, H], H]. \quad (3)$$

The commutators involving the J term of the Hamiltonian (that contains the $|\sigma_n^z|$) can be more easily evaluated with the help of the general relation

$$[\sigma_n^\pm, f(\sigma_m^z)] = \sigma_n^\pm [f(\sigma_m^z) - f(\sigma_m^z \pm \delta_{n,m})]. \quad (4)$$

Here, $f(\sigma_m^z)$ is an arbitrary function of the operator σ_m^z .

The next step is to evaluate the commutators on the right-hand side of Eq. (3). Then, we consider the classical limit $\sigma \rightarrow \infty$ and replace the spin operators σ_n^z and σ_n^\pm by the c numbers

$$\sigma_n^z \rightarrow \sigma \sin \alpha_n, \quad \sigma_n^\pm \rightarrow \sigma \exp(\pm i \phi_n) \cos \alpha_n. \quad (5)$$

Note that the assumption $\sigma \rightarrow \infty$ does not imply that we exclude the short excursions of the holes. Instead, due to the ‘‘potential’’ J term in the Hamiltonian (2), the long excursions are in fact suppressed as compared to the short ones. In the long-wavelength limit, the discrete variable n can be replaced by a continuous one, which we denote y . Hence,

$$|\phi_{n+1} - \phi_n| = a \left| \frac{\partial \phi}{\partial y} \right| \ll 1, \quad |\alpha_n| = a \left| \frac{1}{\sigma} \frac{\partial u}{\partial y} \right| \ll 1 \quad (6)$$

and the equation of motion (3) acquires the simple wavelike form

$$\left(\frac{\partial^2}{\partial t'^2} - \frac{tJa^2}{\hbar^2} \frac{\partial^2}{\partial y^2} \right) \alpha = 0. \quad (7)$$

Here, t' denotes time and a is the lattice spacing. A more detailed derivation is given in the Appendix.

Due to the differential relation between the α and u variables, $\alpha = (a/\sigma)(\partial u/\partial y)$, the displacement of stripe obeys the same wavelike equation,

$$\left(\frac{\partial^2}{\partial t'^2} - \frac{tJa^2}{\hbar^2} \frac{\partial^2}{\partial y^2} \right) u = 0. \quad (8)$$

This equation describes the long-wavelength oscillations of the stripe around the equilibrium position $u = \text{const}$. The corresponding action reads

$$\mathcal{S}[u(y, t')] = \int_{-\infty}^{\infty} dy \int_0^{\infty} dt' \left[\frac{\hbar^2}{2ta^3} \left(\frac{\partial u}{\partial t'} \right)^2 - \frac{J}{2a} \left(\frac{\partial u}{\partial y} \right)^2 \right]. \quad (9)$$

The problem has then been mapped onto a massive string with linear mass density $\rho = \hbar^2/ta^3$ and elastic tension coefficient $C = J/a$.

Finally, one can observe from Eq. (8) that the long-wavelength elementary excitations of the string are gapless and have the phononlike dispersion relation

$$\omega = ck, \quad (10)$$

with phase velocity $c = a\sqrt{tJ}/\hbar$. We emphasize again that our derivation assumes the validity of a continuum description and hence it holds for the rough phase.

III. THRESHOLD FIELD

Up to now, we have only considered the dynamics of a stripe embedded in an antiferromagnetic background. However, in real systems, we have also to take into account the presence of randomly distributed pointlike impurities that act to pin the lines, leading to a glassy phase with trapped stripes. In order to reduce the pinning barrier, we apply an external electric field perpendicular to the stripe's formation. Then, we determine the threshold field above which the potential barrier vanishes and the stripes can flow through the sample, as in a liquid state.

The free energy describing an elastic string along the y direction, which tends to move due to the action of an externally applied electrical field E competing against the pinning barrier V_{pin} is

$$\mathcal{F}[u(y)] = \int_{-\infty}^{\infty} dy \left[\frac{C}{2} \left(\frac{\partial u}{\partial y} \right)^2 + V_{pin} - \frac{eEu}{a} \right]. \quad (11)$$

The next step now is the evaluation of the pinning potential V_{pin} . Let us consider that the pinning mechanism is produced by the ionized acceptors that sit on a plane parallel to and close to the CuO plane. An impurity with two-dimensional coordinates \vec{R} produces at the position \vec{r} in the CuO plane the Coulomb potential $G(\vec{R} - \vec{r})$,

$$G(\vec{R} - \vec{r}) = \frac{e^2}{\epsilon |\vec{R} - \vec{r}|}. \quad (12)$$

The total potential felt at position \vec{r} on the CuO planes can then be written as

$$V_{pin}(\vec{r}) = \frac{1}{a^2} \int d^2\vec{R} \mathcal{N}(\vec{R}) G(\vec{R} - \vec{r}), \quad (13)$$

where $\mathcal{N}(\vec{R})$ is the number of impurities (zero or one) at the position \vec{R} . Hence, $\mathcal{N}(\vec{R}) = [\mathcal{N}(\vec{R})]^2$. Let us denote the average number of impurities per lattice site $\langle \mathcal{N}(\vec{R}) \rangle = \nu$, where $\langle \dots \rangle$ represents the average over the disordered impurity ensemble and $0 < \nu < 1$. If the impurity distribution is uncorrelated, we can write the density-density correlator as

$$\rho_0 = \langle \mathcal{N}(\vec{R}) \mathcal{N}(\vec{R}') \rangle - \langle \mathcal{N}(\vec{R}) \rangle \langle \mathcal{N}(\vec{R}') \rangle = \nu(1 - \nu) \delta(\vec{R} - \vec{R}'). \quad (14)$$

Its Fourier-transform is a constant for any value of the wave vector \vec{k} , $\rho_0(\vec{k}) = \nu(1 - \nu) = \text{const}$. This correlator describes long-wavelength fluctuations with any k , including the small ones. Although the small- k fluctuations are allowed by the statistics of the completely disordered state, in reality they are strongly suppressed by the long-range Coulomb interaction of the impurities, since such fluctuations provide a large value of the Coulomb energy $\sim k^{-1}$. Hence, the real correlator should be suppressed for small k at some scale $k < \lambda$. This cutoff can be introduced by the following choice of the correlation function:

$$\rho(\vec{k}) = \frac{\nu(1 - \nu)}{1 + \lambda^2/k^2}. \quad (15)$$

Since the only length scale in the system of the impurities is the average distance between two neighbor impurities $u = a\nu^{-1/2}$, the λ parameter should be estimated as $\lambda \sim 1/u$. Furthermore, the two-point correlator of the impurity potential is given by

$$\begin{aligned} \mathcal{K}(\vec{r}) &= \langle V_{pin}(\vec{r}) V_{pin}(0) \rangle_d - \langle V_{pin}(\vec{r}) \rangle_d \langle V_{pin}(0) \rangle_d \\ &= \frac{1}{a^4} \int d^2\vec{R} d^2\vec{R}' G(\vec{R}') G(\vec{R} - \vec{r}) \rho(\vec{R}, \vec{R}'). \end{aligned}$$

The Fourier transform of $\mathcal{K}(\vec{r})$ reads

$$\mathcal{K}(\vec{k}) = G^2(\vec{k}) \rho(\vec{k}) = (\nu - \nu^2) \left(\frac{e^2}{\epsilon a} \right)^2 \frac{4\pi^2}{(k^2 + \lambda^2)a^2}, \quad (16)$$

where $G(\vec{k}) = 2\pi e^2/(\epsilon k)$ is the 2D Fourier transform of the Coulomb potential $G(\vec{r})$. Rewriting then the correlator of the potential in real space we find

$$\mathcal{K}(\vec{r}) = 2\pi \left(\frac{e^2}{\epsilon} \right)^2 (\nu - \nu^2) K_0(\lambda r), \quad (17)$$

where $K_0(\lambda r)$ is the modified Bessel function.

Let us now define $\varepsilon_{pin} = \int dy V_{pin}$. If the stripe interacting with the random pinning potential is stiff, the average pinning energy $\langle \varepsilon_{pin}(L) \rangle_d$ of a segment of length L is zero. The fluctuations of the pinning energy, however, remain finite,

$$\langle \varepsilon_{pin}^2 \rangle_d = \frac{1}{a^2} \int_0^L dy \int_0^L dy' \mathcal{K}(0, y-y') \approx \gamma L \quad (18)$$

with

$$\gamma = \frac{2\pi^2 \varepsilon_c^2 \sqrt{\nu}}{a}. \quad (19)$$

Here, $\varepsilon_c = e^2/\epsilon a$ denotes the Coulomb energy scale. The sublinear growth of $\langle \varepsilon_{pin}^2(L) \rangle_d^{1/2}$ is due to the competition between individual pinning centers. The dynamic approach to this problem was introduced by Larkin and Ovchinnikov²⁵ in the ‘‘collective pinning theory’’ (CPT) for describing the dynamics of weakly pinned vortex lines in the high-temperature superconductors. A scaling approach was also considered in connection with the pinning problem in charge-density-wave systems.^{26,27} The results of the CPT can be summarized as follows:²⁸ Equation (18) implies that a stiff stripe is never pinned, since the pinning force grows only sublinearly, whereas the electric driving force increases linearly with length. On the other hand, due to the elasticity, the stripe can accommodate to the potential on some ‘‘collective pinning length’’ L_c . Hence, each segment L_c of the stripe is pinned independently and the driving force is balanced.

Our task now is to determine this length L_c . The evaluation of the free energy by using dimensional estimates provides

$$\mathcal{F}[u, L] \sim C \frac{u^2}{L} - \sqrt{\gamma L} - \frac{eEuL}{a}. \quad (20)$$

By minimizing $\mathcal{F}[u, L]/L$ with respect to L at zero-bias field,²⁸ we determine the collective pinning length L_c along the string,

$$\frac{\delta \mathcal{F}/L}{\delta L} \Big|_{L_c} = 0, \quad L_c \approx \left(\frac{Cu^2}{\sqrt{\gamma}} \right)^{2/3}. \quad (21)$$

Assuming that $u \sim \lambda^{-1} \sim a/\sqrt{\nu}$, the average impurity spacing, and using Eq. (19) we find

$$L_c \approx a \nu^{-5/6} \left(\frac{\varepsilon_l}{\varepsilon_c} \right)^{2/3}, \quad (22)$$

where the elastic energy $\varepsilon_l = Ca$. Experimentally, it is difficult to measure the collective length L_c . However, the threshold electric field E_c corresponding to the vanishing of the barrier is a quantity that can be easily experimentally

determined. The critical value E_c can be estimated by equating the pinning energy $\sqrt{\gamma L_c}$ to the electric energy $eEuL_c/a$. We then obtain

$$E_c = \frac{a}{eu} \sqrt{\frac{\gamma}{L_c}} \sim \frac{\nu^{7/6} \varepsilon_c}{ea} \left(\frac{\varepsilon_c}{\varepsilon_l} \right)^{1/3}. \quad (23)$$

For typical high- T_c materials, such as $\text{La}_{2-\nu}\text{Sr}_\nu\text{CuO}_4$, $J \approx 0.1$ eV, $a \approx 4$ Å, and $\epsilon = \epsilon_0 \approx 30$.²⁹ Hence, one can estimate the elastic energy $\varepsilon_l = J \approx 0.1$ eV and the Coulomb energy $\varepsilon_c = e^2/(\epsilon a) \approx 0.1$ eV. For a doping concentration in the antiferromagnetic insulating phase, for instance, for $\nu = 10^{-3}$, we then obtain the collective pinning length $L_c \approx 10^3$ Å and the critical electrical field $E_c \approx 10^3$ V/cm.

IV. CLASSICAL AND QUANTUM RELAXATION PROCESS

We have estimated the threshold field E_c corresponding to the onset of the motion of depinned stripes. Next, we are interested in studying the relaxation process taking place at applied fields $E < E_c$. In this case there is a finite pinning barrier preventing the motion of the stripe, but it can still jump over (under) the barrier due to thermal (quantum) fluctuations.

A. Classical limit

At high temperatures T , the decay rate Γ_t is given by the Arrhenius law, $\Gamma_t \sim \exp(-U/T)$. The activation energy U can be determined by extremizing the free energy. In other words, within the semiclassical approximation, the energy barrier U is nothing but the free energy \mathcal{F} evaluated at the saddle-point configuration u_s , $U = \mathcal{F}[u_s]$. As far as we are interested in evaluating the decay rate only within exponential accuracy, we can safely neglect the dynamical terms (as for instance, the kinetic one) in the free energy, since these terms would give a correction only to the prefactor multiplying the exponential function.

By substituting the collective length L_c as given by Eq. (22) into the free energy (20), we can estimate the collective pinning energy barrier

$$U_c \approx \sqrt{\gamma L_c} \approx \nu^{-1/6} (\varepsilon_l \varepsilon_c^2)^{1/3}. \quad (24)$$

For the case of $\text{La}_{2-\nu}\text{Sr}_\nu\text{CuO}_4$ with $\nu = 10^{-3}$ considered in the previous section, we estimate the pinning barrier to be of the order of 10^3 K. The barrier exhibits a weak dependence on the doping parameter, $U_c \propto \nu^{-1/6}$. Notice that this barrier height is compatible with the estimates presented in Ref. 20 for the binding energy of holes in a domain wall. Besides, this value is also comparable to the one obtained for the vortex creep process in high- T_c superconductors, when $U_c \sim 10^2 - 10^3$ K.

The dynamics of the stripe in the presence of the pinning potential is simply an example of the more general problem of elastic manifolds in quenched random media. Investigations of the statistical mechanics of this object have shown that a stripe confined to move in a plane is always in a pinned phase,

$$\langle\langle [u(L) - u(0)]^2 \rangle\rangle \sim u_c^2 \left(\frac{L}{L_c}\right)^{2\zeta}, \quad L > L_c, \quad (25)$$

with a wandering exponent $\zeta = \frac{2}{3}$.^{30,31} Here, $\langle\langle \dots \rangle\rangle$ denotes the full statistical average over dynamical variables (thermal) and over disorder, L is the distance along the stripe, and u_c and L_c are transverse and longitudinal scaling parameters, respectively. In our case, $u_c \sim \lambda^{-1}$ (scale of the disorder potential) and L_c is the collective pinning length.

It was also found that competing metastable states that differ from one another on a length L are separated by a distance

$$u(L) \sim u_c \left(\frac{L}{L_c}\right)^\zeta, \quad L > L_c \quad (26)$$

and a typical energy barrier

$$\mathcal{U}(L) \sim U_c \left(\frac{L}{L_c}\right)^{2\zeta-1}, \quad L > L_c, \quad (27)$$

where U_c denotes the scaling parameter for energy. For the single stripe problem, U_c reduces to the collective pinning energy. The free-energy functional at low driving fields $E \ll E_c$ is

$$\mathcal{F}(L) \sim U_c \left(\frac{L}{L_c}\right)^{2\zeta-1} - \frac{eEL_c u_c}{a} \left(\frac{L}{L_c}\right)^{\zeta+1}. \quad (28)$$

The problem now has been reduced to a nucleation process.³² If a nucleus with length L larger than some optimal length L_{opt} is formed, the system will move to the next minimum. On the other hand, if the activated segment is smaller than the optimal one, the nucleus will collapse to zero. The optimal nucleus can be found by extremizing the free energy, $\partial_L \mathcal{F}(L)|_{L=L_{opt}} = 0$ and we obtain

$$L_{opt}(E) \sim L_c \left(\frac{E_c}{E}\right)^{1/(2-\zeta)}. \quad (29)$$

Inserting Eq. (29) back into the free energy (28) we verify that the minimal barrier for creep increases algebraically for decreasing bias field,

$$U(E) \sim U_c \left(\frac{E_c}{E}\right)^\mu \quad (30)$$

with $\mu = (2\zeta - 1)/(2 - \zeta) = \frac{1}{4}$. Hence, the system is in a glassy phase, with a diverging barrier in the limit of vanishingly small applied electric fields.

Another interesting limit to study the dynamical behavior of the stripe is at fields below but close to the critical field E_c , i.e., at $E_c - E \ll E_c$. In this case, the effective potential given by the pinning and the bias electrical field terms can be written as²⁸

$$V_{eff}(u) = V_F \left[\left(\frac{u}{u_F}\right)^2 - \left(\frac{u}{u_F}\right)^3 \right] \quad (31)$$

with $V_F \sim V_c(1 - E/E_c)^{3/2}$ and $u_F \sim u_c(1 - E/E_c)^{1/2}$. The critical potential barrier $V_c = eE_c u_c/a$. The energy of a distortion u_F of the stripe on a scale L_F is estimated to be

$$\mathcal{E}(u_F, L_F) \sim \left[\frac{C}{2} \left(\frac{u_F}{L_F}\right)^2 + V_{eff}(u_F) \right] L_F. \quad (32)$$

The competition between the barrier to be overcome, V_F , and the elastic energy density Cu_F^2/L_F^2 determines the length of the saddle-point configuration

$$L_{FS} \sim u_c \sqrt{\frac{C}{V_c}} \left(1 - \frac{E}{E_c}\right)^{-1/4} \sim L_c \left(1 - \frac{E}{E_c}\right)^{-1/4}. \quad (33)$$

Finally, the energy barrier for thermal activation of the stripe out of the pinning potential reads

$$U(E) \sim u_c V_c \left(\frac{C}{V_c}\right)^{1/2} \left(1 - \frac{E}{E_c}\right)^{5/4} \sim U_c \left(1 - \frac{E}{E_c}\right)^{5/4}. \quad (34)$$

Equations (30) and (34), together with Eq. (24) are the main results of this section. From the experimental point of view, it would be easier to observe the creep of the stripe near criticality, where the thermal process is described by Eq. (34) and the activation barrier (24) can be reduced by one or two orders of magnitude due to the presence of the bias electric field.

B. Quantum limit

At low temperatures, we expect the decay process to be driven by quantum fluctuations. In this case, the dynamical terms become essential since they are related to the so-called traversal time. The tunneling rate is then $\Gamma_q \sim \exp(-B/\hbar)$, where B is given by the Euclidean action S_E of the system (the action in the imaginary time formalism) evaluated at the saddle-point solution, $B = S_E[u_s]$. The total Euclidean action describing the elastic domain wall in the presence of random impurities and an external electric field is

$$S_E[u(y, \tau)] = \int_{-\infty}^{\infty} dy \int_0^{\infty} d\tau \left[\frac{\rho}{2} \left(\frac{\partial u}{\partial \tau}\right)^2 + \frac{C}{2} \left(\frac{\partial u}{\partial y}\right)^2 + V_{pin} - \frac{eEu}{a} \right]. \quad (35)$$

The tunneling time τ_c can be estimated by equating the kinetic and elastic terms,

$$\rho \frac{u_c^2}{\tau_c^2} \sim C \frac{u_c^2}{L_c^2}. \quad (36)$$

We then obtain $\tau_c \sim L_c \sqrt{\rho/C}$. Substituting τ_c into the Euclidean action (35), we find

$$B_c^m \sim \tau_c L_c \frac{Cu_c^2}{L_c^2} \sim u_c^2 \sqrt{\rho C} \sim \frac{\hbar}{v} \sqrt{\frac{\epsilon_l}{t}}. \quad (37)$$

It is important to notice that the extremal value of the action B_c^m does not depend on the collective pinning length L_c and hence it is independent of the pinning potential.

Next, we account for dissipation effects in order to generalize our model. Since we cannot determine the friction coefficient η from microscopic calculations (we are considering frozen Néel phases for describing the antiferromagnetic

background), we will evaluate it in a phenomenological way. Moreover, we restrict ourselves to the simplest case of ohmic dissipation and study the problem within the framework of the Caldeira-Leggett model.³³

In the overdamped limit, when $\eta\tau_c/\rho \ll 1$, we can neglect the massive term in Eq. (35) and substitute

$$\frac{\rho}{2} \left(\frac{\partial u}{\partial \tau} \right)^2 \rightarrow \int_0^\infty d\tau' \frac{\eta_l}{4\pi} \left[\frac{u(\tau) - u(\tau')}{\tau - \tau'} \right]^2. \quad (38)$$

The tunneling time can now be obtained by comparing the dissipative and elastic terms. It reads $\tau_c^\eta \sim \eta_l L_c^2 / C$ and the corresponding minimal action for the tunneling process is

$$B_c^d \sim \tau_c^\eta L_c \frac{Cu_c^2}{L_c^2} \sim \eta_l u_c^2 L_c. \quad (39)$$

Now, we replace the physical quantities in the estimated expressions by their numerical values in order to improve the understanding of our results. The friction coefficient per unit length $\eta_l = \eta/a$ can be estimated from the known data for the metallic phase ($\nu = 0.1$). By using the Drude formula, we can evaluate $\eta = ne^2/\sigma$ and the corresponding relaxation time $\tau = m/\eta$. Here, n is the hole concentration per unitary volume V_0 , $n = \nu/V_0 \sim 10^{-1}/200 \text{ \AA}^3 = 0.5 \times 10^{21} \text{ cm}^{-3}$, σ is the normal-state conductivity, $\sigma \sim 10^3 \text{ \Omega}^{-1} \text{ cm}^{-1}$ (Ref. 34), and m is the effective tight-binding mass of the carriers in the CuO plane, $m/m_e \sim 1$,³⁵ with m_e denoting the free-electron mass. We then obtain $\eta \sim 10^{-13} \text{ g/s}$ and $\tau \sim 10^{-14} \text{ s}$. The relaxation time is assumed to be independent of the doping, and to have the same order of magnitude for the metallic and insulating states. The tunneling time $\tau_c \sim 10^{-12} \text{ s}$ and $\tau_c^\eta \sim 10^{-10} \text{ s}$. This indicates that the quantum dynamics is overdamped, and that a proper theory for describing the relaxation process should account in a more accurate way for the dissipative term.

Let us now calculate the correction to the minimal action due to the presence of the electric field. In general, a quantum d -dimensional problem can be regarded as a classical $(d+1)$ -dimensional problem, with the imaginary time being considered as the additional dimension. However, one should notice that the disorder potential fluctuates in space, but not in time. At high temperatures, the stripe jumps over the barrier and the time needed for the jump is irrelevant. At low temperatures, instead, this time is essential. Hence, for the classical motion the stripe can choose optimal barriers [see Eq. (27)], whereas for tunneling the relevant barrier scales like the average barrier $U_c(L/L_c)$ (see Ref. 28 for a more detailed discussion). As a consequence, we obtain that in the limit of low driving fields $E \ll E_c$, the minimal action reads

$$B \sim B_c \left(\frac{E_c}{E} \right)^{\mu_q}, \quad (40)$$

where $\mu_q = (1 + \zeta)/(2 - \zeta)$ and B_c is B_c^m or B_c^d [given by Eqs. (37) or (39), respectively], depending if we are considering the massive or the dissipative limits. Remembering that in our case $\zeta = \frac{2}{3}$, we finally obtain a quantum glassy expo-

nent $\mu_q = \frac{5}{4}$. Near criticality, the results change considerably: as in the thermal case, the quantum action exhibits in this limit a power-law behavior,

$$B \sim B_c \left(1 - \frac{E}{E_c} \right)^\alpha, \quad (41)$$

with $\alpha = 1$ for the massive stripe and $\alpha = \frac{3}{4}$ for the overdamped one.

V. DISCUSSIONS

In this work we have succeeded in deducing a wavelike equation for the motion of a line of holes embedded in an antiferromagnetic phase, which we have chosen to describe by a t - J model. This was done through the application of semiclassical methods to a fictitious spin chain whose local spins can appropriately be related to the difference between the displacements of neighboring holes along a direction perpendicular to the line itself. Therefore we were able to establish a connection between the microscopic parameters of the t - J model and the phenomenological mass and elastic coefficients of the continuum theory by using the fictitious spin model as an intermediate step.

We have also extended the well-established ‘‘collective pinning theory,’’ which has successfully been applied to vortices in superconductors and charge density waves in quasi-1D electronic systems, to the case of the wall of holes. In so doing, we were able to estimate the threshold field for the depinning of the wall as well as the energy barrier per unit length felt by the trapped line. These quantities allowed us to compute the thermal and quantal rates for the depinning of a single wall of holes.

These results can be tested by measuring the conductance of a sample, which presents the striped phase in its antiferromagnetic regime, as a function of the external field (voltage). From our findings, we expect to have a vanishingly small conductance up to the threshold field and then a gradual tendency to recover the ohmic regime for $E > E_c$. This highly nonlinear behavior of the conductance is analogous to that observed in charge-density-wave systems.³⁶ It is also important to notice that in order to compare our results with the experimental ones, one should take into account that inhomogeneities in the barrier height distribution may affect the observed threshold field. Actually, the measured value is a lower bound for the estimated voltage, and results differing by even one order of magnitude from our findings would not be surprising.

Finally, we would like to say some words about our approach to the damping of the wall motion. We have chosen to use an entirely phenomenological approach to the problem because it is not possible to describe dissipation from the present microscopic model. The first step in this direction would be to allow the spin system to respond to any change of the line configuration, i.e., we should assume a finite stiffness for the magnetic system. We plan to proceed further along this direction in a future publication.

ACKNOWLEDGMENTS

We are indebted to M. Balaña, D. Baeriswyl, A. H. Castro Neto, and H. Schmidt for fruitful discussions. This work was

supported by the DAAD-CAPES project number 415-probral/schü (Germany) and 053/97 (Brazil). N.H. acknowledges financial support from the Gottlieb Daimler- und Karl Benz- Stiftung and the Graduiertenkolleg ‘‘Physik nanostrukturierter Festkörper,’’ Universität Hamburg. Y.D. acknowledges financial support from the Otto Benecke-Stiftung. A.O.C. was also partly supported by CNPq

(Conselho Nacional de Desenvolvimento Científico e Tecnológico/Brazil).

APPENDIX

Our aim here is to calculate the commutators on the right-hand side of Eq. (3). With the help of the relation (4), one obtains

$$\begin{aligned} \hbar^2 \ddot{\sigma}_n^z &= -[[\sigma_n^z, H], H] \\ &= \frac{tJ}{\sigma^2} \{ (\sigma_n^+ \sigma_{n+1}^-) (|\sigma_{n+1}^z| + |\sigma_n^z| - |\sigma_{n+1}^z - 1| - |\sigma_n^z + 1|) - (\sigma_n^- \sigma_{n+1}^+) (|\sigma_{n+1}^z| + |\sigma_n^z| - |\sigma_{n+1}^z + 1| - |\sigma_n^z - 1|) \\ &\quad + (\sigma_n^+ \sigma_{n-1}^-) (|\sigma_{n-1}^z| + |\sigma_n^z| - |\sigma_{n-1}^z - 1| - |\sigma_n^z + 1|) - (\sigma_n^- \sigma_{n-1}^+) (|\sigma_{n-1}^z| + |\sigma_n^z| - |\sigma_{n-1}^z + 1| - |\sigma_n^z - 1|) \} \\ &\quad + \frac{2t^2}{\sigma^4} \{ \sigma_{n+1}^z (\sigma_n^+ \sigma_n^- + \sigma_n^- \sigma_n^+ + \sigma_n^+ \sigma_{n+2}^- + \sigma_n^- \sigma_{n+2}^+) + \sigma_{n-1}^z (\sigma_n^+ \sigma_n^- + \sigma_n^- \sigma_n^+ + \sigma_n^+ \sigma_{n-2}^- + \sigma_n^- \sigma_{n-2}^+) \\ &\quad - \sigma_n^z (\sigma_{n+1}^+ \sigma_{n+1}^- + \sigma_{n+1}^- \sigma_{n+1}^+ + \sigma_{n-1}^+ \sigma_{n-1}^- + \sigma_{n-1}^- \sigma_{n-1}^+ + 2\sigma_{n-1}^+ \sigma_{n+1}^- + 2\sigma_{n-1}^- \sigma_{n+1}^+) \}. \end{aligned}$$

Now, we consider the problem in the classical limit, when the operators σ_n^z and σ_n^\pm can be replaced by c numbers. In spherical coordinates, we can write

$$\sigma_n^z = \sigma \sin \alpha_n, \quad \sigma_n^\pm = \sigma \exp(\pm i \phi_n) \cos \alpha_n, \quad (\text{A1})$$

where $\alpha_n = \pi/2 - \theta_n$. Using that $\phi_n - \phi_{n-1} \sim 0$ and $\sigma_n^z \ll 1$, we obtain the classical equation of motion

$$\hbar^2 \ddot{\alpha}_n = t \left(J + \frac{8t}{\sigma^2} \right) (\alpha_{n+1} - 2\alpha_n + \alpha_{n-1}). \quad (\text{A2})$$

Further, we take the limit $\sigma \rightarrow \infty$ and go to the continuous approximation. In this limit, we can replace

$$\alpha_n \rightarrow \alpha(y), \quad \alpha_{n\pm 1} \rightarrow \alpha(y) \pm a \alpha'(y) + \frac{a^2}{2} \alpha''(y), \quad (\text{A3})$$

and we eventually obtain the wavelike equation

$$\left(\frac{\partial^2}{\partial t'^2} - \frac{tJ a^2}{\hbar^2} \frac{\partial^2}{\partial y^2} \right) \alpha = 0. \quad (\text{A4})$$

¹H. J. Schulz, Phys. Rev. Lett. **64**, 1445 (1990).

²D. Poilblanc and T. M. Rice, Phys. Rev. B **39**, 9749 (1989).

³M. Inui and P. B. Littlewood, Phys. Rev. B **44**, 4415 (1991).

⁴J. Zaanen and O. Gunnarsson, Phys. Rev. B **40**, 7391 (1989).

⁵V. L. Pokrovsky and A. L. Talapov, in *Theory of Incommensurate Crystals*, edited by I. M. Khalatnikov (Hardwood Academics, Chur, Switzerland, 1984), Vol. 1.

⁶T. Giamarchi and C. L. Huillier, Phys. Rev. B **42**, 10 641 (1990).

⁷P. Prelovsek and X. Zotos, Phys. Rev. B **47**, 5984 (1993).

⁸J. M. Tranquada, D. J. Buttrey, V. Sachan, and J. E. Lorenzo, Phys. Rev. Lett. **73**, 1003 (1994).

⁹V. Sachan, D. J. Buttrey, J. M. Tranquada, J. E. Lorenzo, and G. Shirane, Phys. Rev. B **51**, 12 742 (1995).

¹⁰J. M. Tranquada, J. E. Lorenzo, D. J. Buttrey, and V. Sachan, Phys. Rev. B **52**, 3581 (1995).

¹¹J. Zaanen and P. B. Littlewood, Phys. Rev. B **50**, 7222 (1994).

¹²J. M. Tranquada, B. J. Sternlieb, J. D. Axe, Y. Nakamura, and S. Uchida, Nature (London) **375**, 561 (1995); J. M. Tranquada, J. D. Axe, N. Ichikawa, Y. Nakamura, S. Uchida, and B. Nachumi, Phys. Rev. B **54**, 7489 (1996); J. M. Tranquada, J. D. Axe, N. Ichikawa, A. R. Moodenbaugh, Y. Yakamura, and S. Uchida,

Phys. Rev. Lett. **78**, 338 (1997).

¹³T. E. Mason, A. Schroder, G. Aeppli, H. A. Mook, and S. M. Hayden, Phys. Rev. Lett. **77**, 1604 (1996).

¹⁴K. Yamada, C. H. Lee, Y. Endoh, G. Shirane, R. J. Birgeneau, and M. A. Kastner, Physica C **282-287**, 85 (1997).

¹⁵F. Borsa, P. Carretta, J. H. Cho, F. C. Chou, Q. Hu, D. C. Johnston, A. Lascialfari, D. R. Torgeson, R. J. Gooding, N. M. Salem, and K. J. E. Vos, Phys. Rev. B **52**, 7334 (1995).

¹⁶A. H. Castro Neto and D. Hone, Phys. Rev. Lett. **76**, 2165 (1996).

¹⁷A. H. Castro Neto, Phys. Rev. Lett. **78**, 3931 (1997).

¹⁸T. M. Rice, in *High Temperature Superconductivity*, Proceedings of the 39th Scottish Universities Summer School in Physics, edited by D. P. Turnstall and W. Barford (Adam Hilger, London, 1991), p. 317.

¹⁹S. R. White and D. J. Scalapino, Phys. Rev. Lett. **80**, 1272 (1998).

²⁰J. Zaanen, M. L. Horbach, and W. van Saarloos, Phys. Rev. B **53**, 8671 (1996); J. Zaanen and W. van Saarloos, cond-mat/9702060 (unpublished).

²¹N. Hasselmann, A. H. Castro Neto, C. Morais Smith, and Yu. Dimashko (unpublished).

²²H. Eskes, R. Grimberg, W. van Saarloos, and J. Zaanen, Phys.

- Rev. B **54**, 724 (1996); H. Eskes, O. Y. Osman, R. Grimberg, W. van Saarloos, and J. Zaanen (unpublished).
- ²³M. den Nijs and K. Rommelse, Phys. Rev. B **40**, 4709 (1989).
- ²⁴H. J. Schulz, Phys. Rev. B **34**, 6372 (1986).
- ²⁵A. I. Larkin and Yu. N. Ovchinnikov, Zh. Eksp. Teor. Fiz. **65**, 1704 (1973) [Sov. Phys. JETP **38**, 854 (1974)]; J. Low Temp. Phys. **34**, 409 (1979).
- ²⁶H. Fukuyama and P. A. Lee, Phys. Rev. B **17**, 535 (1978).
- ²⁷P. A. Lee and T. M. Rice, Phys. Rev. B **19**, 3970 (1979).
- ²⁸G. Blatter, M. V. Feigel'man, V. B. Geshkenbein, A. I. Larkin, and V. M. Vinokur, Rev. Mod. Phys. **66**, 1125 (1994).
- ²⁹C. Y. Chen, N. W. Preyer, P. J. Picone, M. A. Kastner, H. P. Jenssen, D. R. Gabbe, A. Cassanho, and R. J. Birgeneau, Phys. Rev. Lett. **63**, 2307 (1989).
- ³⁰D. A. Huse, C. L. Henley, and D. S. Fisher, Phys. Rev. Lett. **55**, 2924 (1985).
- ³¹M. Kardar, Nucl. Phys. B **290**, 582 (1987).
- ³²J. S. Langer, Ann. Phys. (Leipzig) **41**, 108 (1967).
- ³³A. O. Caldeira and A. Leggett, Ann. Phys. (N.Y.) **149**, 374 (1983).
- ³⁴R. J. Cava, R. B. van Dover, B. Batlogg, and E. A. Rietman, Phys. Rev. Lett. **58**, 408 (1987).
- ³⁵L. F. Mattheiss, Phys. Rev. Lett. **58**, 1028 (1987).
- ³⁶J. H. Miller, Jr., J. Richard, J. R. Tucker, and J. Bardeen, Phys. Rev. Lett. **51**, 1592 (1983).